

Stable data-driven manufacturing decision making by introducing causal relationships for high dimensional data

Abstract—In digital manufacturing, data-driven methods are promising to revolutionize various decision-making processes. However, the relationships between variables in high-dimensional data of data-driven decision-making methods are only correlations. Important causal relationships and knowledge between process variables are not considered. Therefore, existing data-driven systems are instable, which could result in unreliable and dangerous decisions. To establish a stable decision-making model for complex processes with high-dimensional data, a causal-based decision-making framework combined causal relationships and knowledge between key manufacturing variables was proposed. The causal relationships between State, Decision and Objective data was established in form of direct acyclic graph forming by breaking an unexcepted loop between variables using a Shadow Objective variable. Then, causal knowledge of high-dimensional state was introduced to the neural network, forming a stable decision-making model. Compared with data-driven methods used in robotics and manufacturing scenarios, the proposed framework provided better and stable decisions particularly in noised environments.

Index Terms—Manufacturing decision-making, Data-driven, Causal relationship, Causal loop.

I. INTRODUCTION

In intelligent manufacturing, decision making systems strive to leverage data gathered throughout the product lifecycle for making optimized decisions quickly in complex environments [1], leading to cost reduction and improved product quality [2]. These systems make decisions based on specific requirements in particular situations, e.g., a state of manufacturing at certain moment, which can be reflected by captured data including images, sounds and other forms of signals from environment. The complexity of modern

manufacturing scenarios, characterized by high-dimensional and noisy data, poses stability challenges. Decision making with respect to states is still a challenging research area [3].

Manufacturing decision making depends on the deep understanding of manufacturing systems including capabilities, mechanisms, knowledge and human experience. Existing decision making methods can be broadly classified into three categories (as summarized in Table 1), i.e., (i) Knowledge based approach, relying on expert knowledge including production rules extracted by human or algorithms, like fuzzy logic algorithms [4], [5], [6]; (ii) Mechanism Model based approach, relying on the modelling of physical systems and integrated optimization, like genetic algorithms [7], Monte-Carlo simulation [8] and ant colony optimization [9]; and (iii) Data-driven approach, relying on data mining technologies [10], extracting knowledge using machine learning algorithms [11]. In practice, both the knowledge and mechanism model based decision making methods were inefficient and ineffective in ensuring decision quality and stability particularly when dealing with complex manufacturing scenarios with high-dimensional data [12].

In the Industry 4.0 era, data-driven methods and deep learning techniques have emerged as powerful tools to revolutionize intelligent manufacturing by utilizing rich data for optimized solutions [13], [14]. Data-driven decision-making methods have mainly two types, i.e., reinforcement learning [15] and supervised learning [16]. Reinforcement learning focuses on learning optimal decisions to maximize rewards by experience accumulated from interactions with the environment, e.g., the multi-actor networks for decision making in changing environment proposed by Liu et.al [17]. Reinforcement learning has limitations in designing reward function and the efficiency in interactions with environment.

TABLE 1
PEARSON COEFFICIENTS OF EACH PAIRS OF ACTION ERRORS

Category of existing methods	References	Comments
Knowledge-based	[4,5,6]	Relied on expert knowledge and production rules to make decisions. Provided a foundation for rule-based decision-making systems.
Mechanism Model-based	[7,8,9]	Used physical system modeling and integrated optimization methods. Enhanced the understanding of optimization processes.
Data-driven:		
Reinforcement Learning	[15,17]	Learned optimal decisions by maximizing rewards through interactions with the environment. Suitable for dynamic and complex decision-making scenarios.
Supervised Learning	No causal [11,16,19,20]	Learned mappings between input data and output decisions, and avoided non-stationary learning process complexity.
	Causal This paper	Developed robust causal supervised learning models that account for environmental noise and changes, enhancing decision accuracy.

Supervised learning is a deep learning framework for decision making [18], e.g., the supervised learning approach for decision making developed by Jurgen [19] and Rupesh et al. [20]. Supervised learning includes agents which learn the mapping between the input data and the corresponding output decision labels, so that optimized decisions can be made on new, unseen data. Unlike reinforcement learning, supervised learning avoids the complexity of non-stationary learning process and offers greater interpretability.

Existing data-driven decision-making methods, only extract the correlations [21], which are statistics relationships among variables on the training data. However, when the data distribution is altered by environmental noises or changes, models based on statistical relationships are prone to failure, leading to erroneous decisions. This theoretical problem imposed a challenge for deploying data-driven systems in practical decision making [22], e.g., when noised data in images and sensor signals was used for planning robot tasks, it can lead to incorrect decisions on robot movements.

This research investigated the above limitations in current data-driven decision-making methods and identified a crucial factor that affected their accuracy and stability: the underutilization of causal relationships between variables. Causal relationships are becoming increasingly vital for models in industrial environments. In the prediction aspect, Li et al. [23] proposed a causal consistency network to learn unchanging causal relationships across different datasets to improve the generalization of bearing fault diagnosis models. In decision making aspect, the causal relationships between variables are the knowledge that humans relying on, e.g., a motion instruction (decision) is determined (caused) by the target position (objective) that a robot end effector needs to reach the current position (state). This essential knowledge is often absent or not considered in current data-driven manufacturing decision-making methods.

To address this problem, a causal based data-driven decision making framework was proposed and developed in this research, in which underlying causal relationships between key manufacturing variables are modelled with associated knowledge. The accuracy and stability of the method in the proposed framework was tested and compared with typical data-driven methods without causal knowledge in two case studies: one for robotics reach task (using simulation), and the other for manufacturing deformation control task (using simulation and real experiment) under various noises from the environments. The results indicated that, in both tasks, the decision making models incorporating causal knowledge demonstrated higher accuracy and stability (measures of accuracy and stability are explained and demonstrated in the case study Section). The main contributions of this research include the following:

- 1) A causal-based data-driven decision making method was proposed, in which the decision making problem in manufacturing is defined from causal perspectives. A shadow objective variable, replacing the objective variable, is introduced to break the loop among variables in causal graph, in which the loop would

cause unstable model. From the reported research, this was the first attempt to tackle the loop influence on decision making causal graphs.

- 2) The causal knowledge and intervention are formulated in the neural network of decision making framework by an adjacency matrix and a mask mechanism. It helps decouple the input high-dimensional data and achieve stable decision making in noisy environments.
- 3) The proposed causal based decision making method was applied to the two case studies (the robotics motion and deformation control tasks) in noisy manufacturing environments. The effective information [24], [25] (i.e., the extent of the causal influence of the input on the output) was introduced to evaluate the causal learning ability of the neural networks. The results showed that there was a relationship between effective information, causal strength and generalization ability.

II. PROBLEM DEFINITION AND ANALYSIS

This Section will analyze data-driven decision making modeling problems from causal perspective.

A. Overview of the caused-based decision making framework

Existing decision-making systems in intelligent manufacturing leverage data gathered throughout the product lifecycle to optimize decisions. The primary challenges lies in the instability of existing data-driven methods which are often based solely on statistical correlations between variables. Such correlations can be disrupted by environmental noise, leading to unreliable and potentially unsafe decisions. However, in controlled and relatively stable manufacturing environments, there generally exist stable causal relationships among variables from manufacturing system. Our proposed framework integrates these stable causal relationships, extracted from the manufacturing environment, into data-driven decision models, ensuring the stability and reliability of decision-making processes. This section introduces the comprehensive framework utilized in this study. Fig. 1 provides an overview of the proposed causal based decision making framework.

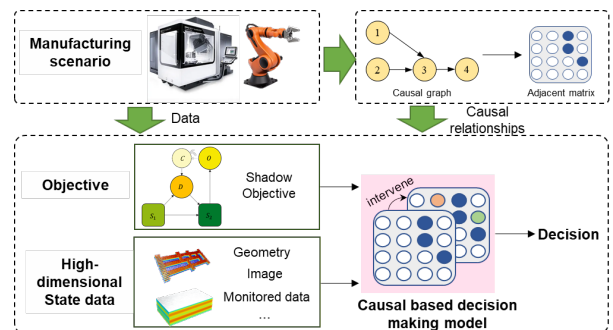


Fig. 1 Overview of the proposed causal based decision making framework

B. Decision making problem definition

Individual decision making aims to make reasonable

Decision D based on current State S and Objective O . For a data-driven decision making model, Decision D is modelled as a variable. For the same state and objective, models at different stages of learning may make different decisions, making the decision process appear stochastic. The goal of the data-driven decision model is to reduce this uncertainty to learn how to make optimal decisions. Thus, the learning objective could be seen as the likelihood function for the decision making model, using the Maximum Likelihood Estimation [26], can be formulated as,

$$\theta^* = \operatorname{argmax}[p(D|O, S; \theta)] \quad (1)$$

where $D \in \mathbb{R}^d$ denotes the Decision variables (decided solution), $S \in \mathbb{R}^s$ denotes the State variables, which is normally high dimensional. $O \in \mathbb{R}^o$ denotes the Objective variables. Parameter θ is the parameter of data-driven model aiming to optimize to get θ^* . It is the weight and bias of the neural network in this paper, which is trained to maximize the likelihood of the observed data given the model. This equation defines a function parameterized by θ that estimates the Decision variables D , based on the State variables S and Objective variables O , as illustrated in Fig. 2.

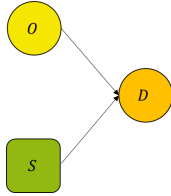


Fig. 2 The relationships between decision making variables.

Maximizing the likelihood function allows the model to produce the most probable output, considering the observed input States and Objectives in training data. It is well known that relying on data posterior to capture causal relations can lead to spurious conclusions. For example, considering the relationship between ice cream sales and swimming drowning accidents, while data analysis might reveal a positive correlation, controlling ice cream sales cannot reduce drowning accidents. Therefore, although current data-driven methods demonstrated ability in capturing the relationships between State variables, Objective variables, and Decision variables, they can only capture the statistics correlations, which is not stable in changing environments, i.e., the correlations are not consistently maintained.

In addition, State variables are typically high dimensional data including a mix of features related and unrelated to Decision making. For the image-driven robot task example, the State variable is made up of numerous pixels, involving Decision-related features (robot's arm and end effector), and features not related to Decision (background noises which disturb decision making). Among all the features in State S , Decision-related features are the critical features as they contain information about how the Decision impacts on the relevant features and on the Objective. Because these features are mixed with other features in pixels, the extraction is very difficult. Learning directly from this kind of incorrect inputs data would lead to poor model stability, especially in changing

environments with noises. Therefore, it is crucial to clearly distinguish the Decision-related features from the high-dimensional data for achieving optimized decision making.

B. Causal based decision making problem definition

From a causal perspective, the decision making problem can be defined as a causal inference problem, with the goal of making optimized Decisions that align with the Objectives using causal knowledge. The process involves identifying potential causes of objectives, estimating the causal effects of these potential causes on the objectives through statistical models, and subsequently making decisions based on these estimated causal relationships.

Let $G = \{V, E\}$ be a direct graph with a node set $V = [v_1, \dots, v_v]$ and edge set $E = [e_1, \dots, e_e]$. This graph serves as a model for depicting the causal relationships among a set of variables. Let \mathbf{Pa}_{v_i} denote the parents of v_i , where parents are the nodes that exert an influence on the child node v_i . The probability of v_i depends on all its parents. If an intervention is acted on node v_i , denoted as $do(v_i = \text{constant } v)$, it would force a change in the value v_i to constant v . This intervention also leads to removal of all edges from \mathbf{Pa}_{v_i} to v_i , because the constant value of v_i is no longer influenced by any other nodes. Consequently, the intervention changes both the graph structure and its probability distribution.

From the causal perspective, the observable data, i.e., the data that can be collected directly from the environment, can be denoted as $\{O, D, S_1, S_2, A\}$ in data-driven decision making, where A is an adjacency matrix, representing the causal relationship of features in high-dimensional State data S .

For decision making in supervised learning, because the Decision D variables are determined by current State S_1 and Objective O , in terms of causal relationship, the causes of Decision D are the current State S_1 and Objective O , i.e., $\mathbf{Pa}_D = \{O, S_1\}$. In this paper, it is assumed that Decision D made by current State S_1 can only affect the next state S_2 , which is the basis of Objective O , i.e., $\mathbf{Pa}_{S_2} = \{D, S_1\}$ and $\mathbf{Pa}_O = \{S_2\}$. Thus, the causal relationships can be represented as a directed graph as shown in Fig. 3 (a).

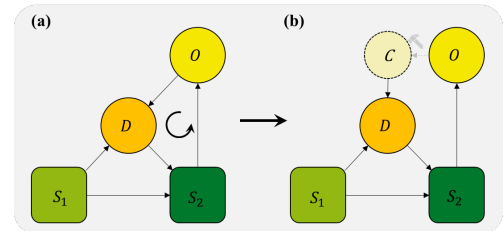


Fig. 3 Causal relationship graph of variables in decision making. (a) a cyclic graph. (b) cyclic loop is broken by introducing a shadow objective variable.

It can be noticed in Fig. 2 (a) that there is a cyclic loop among O , D and S_2 , where Decision D affects State S_2 , State S_2 affects Objective O , and Objective O affects Decision D . This cyclic relationship is reflected in the joint probability distribution of the variables is

$$p(\text{Cyclic}) = p(D|S_1, O)p(S_2|S_1, D)p(O|S_2)p(S_1)$$

$$= p(\mathbf{O}, \mathbf{D}, \mathbf{S}_1, \mathbf{S}_2 | \mathbf{S}_2). \quad (2)$$

Equation (2) highlights that the existence of a cyclic loop results in State variable \mathbf{S}_2 appearing both in the conditions and results of the probability $p(\mathbf{O}, \mathbf{D}, \mathbf{S}_1, \mathbf{S}_2 | \mathbf{S}_2)$. It leads to the presence of non-unique solutions and instability in probability distribution modeling. Therefore, the presence of cyclic loop in causal graph makes it difficult to solve causal models.

Previous researchers have employed several methods to address loops in causal modeling. One type of methods unfolds variables in time-series, where variables are sampled and modeled assuming a balanced distribution, as variable relationships remain stable under such conditions. Karl et al. [27] introduced a common result variable to unfold the causal graph in recommendation systems. For cases where variables can be unfolded in a time sequence but lack a balanced distribution, methods such as Granger causality and cross-mapping [28] can analyze causal relationships between variables, but cannot model causal effects [27]. However, the causal relationship graph in Fig. 2(a) is a directed cyclic graph, making it difficult to unfold it based on time sequence and establish a balanced distribution. As a result, causal modeling in decision models continues to be a challenging problem.

To solve the above problem, this research proposed a method for breaking the loop by introducing an intermediate variable \mathbf{C} , named Shadow Objective variable, to replace the Objective variable \mathbf{O} as the reference for decision making. The Shadow Objective variable equivalently represents the influence of Objective variable on Decision variable \mathbf{D} . Because the Shadow Objective variable is an intermediate variable, there is an edge from \mathbf{O} to \mathbf{C} . By intervening on \mathbf{C} , the loop is broken, and a directed acyclic graph (DAG) is formed, as illustrated in Fig. 3 (b).

Implementation of an intervention on the Shadow Objective variable, i.e., removing the edges directed toward it, rendering the Shadow Objective variable and Objective variable independent. Therefore, the decision making modelling problem transforms into a causal modeling problem with an intervened Shadow Objective variable $do(\mathbf{C})$, as

$$\begin{aligned} & p(\text{Acyclic}) \\ &= p(\mathbf{D} | \mathbf{S}_1, do(\mathbf{C})) p(\mathbf{S}_2 | \mathbf{S}_1, \mathbf{D}) p(\mathbf{O} | \mathbf{S}_2) p(\mathbf{S}_1) p(do(\mathbf{C})) \\ &= p(\mathbf{O}, \mathbf{D}, \mathbf{S}_2, \mathbf{S}_1, do(\mathbf{C})) \end{aligned} \quad (3)$$

where do is the intervention operator. The probability distribution calculation with intervened variable is generally estimated by observable variable data distribution. Following the two invariance equations for causal effect calculation, which are marginal probability invariance equation and the conditional probability invariance equation, the conditional probability can be expressed as $p(\mathbf{D} | \mathbf{S}_1, do(\mathbf{C})) = p(\mathbf{D} | \mathbf{S}_1, \mathbf{C})$. Thus, the causal graph model can be reformulated as,

$$p(\mathbf{O}, \mathbf{D}, \mathbf{S}_2, \mathbf{S}_1, do(\mathbf{C})) = p(\mathbf{O}, \mathbf{D}, \mathbf{S}_2, \mathbf{S}_1, \mathbf{C}). \quad (4)$$

Equation (4) shows that the introducing of a Shadow Objective variable, along with intervening, resulting in a directed acyclic causal graph. Thus, a causal based decision making model can be established by solving the probability.

In causal based decision-making, apart from optimizing the objective as in (1), another crucial objective is to ensure that the chosen solution leads to the state corresponding to Objective \mathbf{O} . Hence, the solving objective is as follows:

$$\theta^* = \operatorname{argmax}[p(\mathbf{D} | \mathbf{C}, \mathbf{S}_1) p(\mathbf{O} | \mathbf{S}_2; \theta) p(\mathbf{S}_2 | \mathbf{S}_1, \mathbf{D}; \theta, \mathbf{A})] \quad (5)$$

where \mathbf{A} is prior known causal relationships between features of State \mathbf{S} , which is represented by adjacency matrix.

In summary, the causal perspective emphasizes the importance of understanding the causal relationships between variables and decisions, which provides a basis for decision making model that can lead to optimal decisions.

III. CAUSAL BASED DECISION MAKING FRAMEWORK

This Section will describe the framework developed on the DAG, to address the studied problem. The framework contains three components: (i) decoupling representation learning achieved by introducing causal relationship of high-dimensional data in neural network, (ii) causal inference modeling and (iii) decision intervention modeling.

A. Decoupling representation learning via causal relationships

In manufacturing processes, State variable \mathbf{S} is mainly high dimensional micro data (such as the pixels in image with robotics), but also contains macro features (such as the robot body made up of pixels), which are more relevant to the applications of the proposed method. Among those macro features, there often exist prior causal relationships. However, these features are mixed within microdata, making extraction challenging and impeding application of causal relationships.

To address this issue, the latent variable and an adjacency matrix were used in this research to represent the macro features and the causal relationships among them. Because the latent variable is a kind of abstract feature of State variable \mathbf{S} , requiring extraction from \mathbf{S} . **Therefore, an encoder module was used to extract features from State variable \mathbf{S} to encode it in a latent space by latent variables \mathbf{Z} , which was the representation of State variable \mathbf{S} . While, a decoder module was used to recover State variable \mathbf{S} from latent space.** Thus, the calculation process between \mathbf{S} and \mathbf{Z} was established by the encoder and decoder modules, respectively.

$$\mathbf{Z} = \operatorname{encoder}(\mathbf{S}). \quad (4)$$

$$\mathbf{S} = \operatorname{decoder}(\mathbf{Z}). \quad (5)$$

The causal relationships between latent variables $\mathbf{Z} \in \mathbf{R}^n$, are formulated by adjacency matrix $\mathbf{A} \in \mathbf{R}^{n \times n}$, where A_{ij} represents the presence of the edge from variable z_i to z_j with value 1 (if there is no edge, the value is 0).

B. Causal inference modeling in neural networks

In the causal inference component of the framework, the transmission of latent variables is modeled. Let structure function $\mathbf{g} = \{g_1, g_2, \dots, g_n\}$, which describes the transmission process from the parent variables to child variables. The transmission process of latent variables can be represented as,

$$z_i = g_i(\mathbf{A}_i \circ \mathbf{Z}_i) \quad (6)$$

where \mathbf{A}_i is the i^{th} row of \mathbf{A} , \circ is the element-wise multiplication, g_i is the function that maps the parent node variables $\mathbf{P}\mathbf{a}_{z_i}$ to node z_i . It encodes the causal effect from the parent node to node z_i . g_i is achieved by neural network.

C. Decision intervention modeling in neural networks

In the causal-based decision making framework, the Decision variable was treated as an intervention on State features represented by latent variable \mathbf{Z} . To accomplish this in neural network, the masking mechanism [29] was introduced to perform interventions using different masks. Because the latent variable \mathbf{Z} can be divided into two types of variables, i.e., Decision-related variables s^D and variables s^{-D} unrelated to Decision. The decision intervention only works on Decision related variables s^D . The implementation of decision intervention is as follows,

$$\mathbf{Z}^{do} = \mathbf{Z}^T \mathbf{do} + \mathbf{V}^{do}, \mathbf{do} = \{m_0, \dots, m_n\}, \mathbf{V}^{do} = \{v_1, \dots, v_n\} \quad (7)$$

$$m_i = \begin{cases} 1, & z_i \in s^{-D} \\ 0, & z_i \in s^D \end{cases} \quad (8)$$

$$v_i = \begin{cases} f_{do}(d_i), & z_i \in s^D \\ 0, & z_i \in s^{-D} \end{cases} \quad (9)$$

where \mathbf{do} is a mask vector composed of a set of binary masks m_i , where each mask determines whether the latent variable z_i is intervened. \mathbf{V}^{do} is the intervention value of the intervened variable, which can be calculated using the Decision variable d_i . These equations are suitable for discrete or continuous Decision variables. The function f_{do} can be established through a neural network.

D. The proposed framework architecture

The proposed causal based data-driven decision making framework is illustrated in Fig. 4.

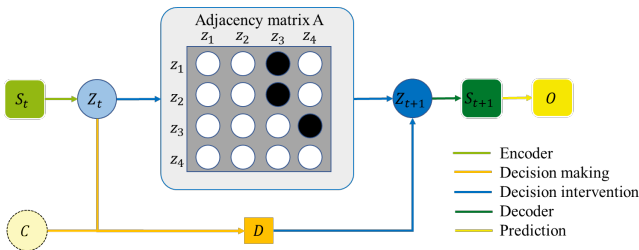


Fig. 4 The proposed causal based decision making framework.

The framework has three components including decoupling representation learning, causal inference, and decision intervention. There are five neural network modules shown in different colours, including encoder, decision making, decision intervention, decoder and prediction modules.

The first module is an encoder which extracts macro features, i.e., Latent variable \mathbf{Z}_t , from State variable \mathbf{S}_t , and takes \mathbf{S}_t as input and outputs \mathbf{Z}_t of the State. The second one is a decision making module which makes decision based on Latent variable \mathbf{Z}_t and Shadow Objective variable \mathbf{C} , and takes \mathbf{Z}_t and \mathbf{C} as input and outputs Decision variable \mathbf{D} . The third one is a decision intervention module which is used to realize causal inference, and takes Latent variable \mathbf{Z}_t and Decision variables as input and produces Latent variables \mathbf{Z}_{t+1} as output, it is generated after the decision is executed. Each causal variable has a function estimated by the neural network that establishes the relationship between parents and child nodes. The fourth module is a decoder which recovers the next State variable \mathbf{S}_{t+1} from Latent variable \mathbf{Z}_{t+1} , and takes \mathbf{Z}_{t+1} as input and reconstructs \mathbf{S}_{t+1} . The fifth one is a prediction module which takes State variable \mathbf{S}_{t+1} as input and outputs Objective variable \mathbf{O} .

The learning objective of the decision making model is to maximize the likelihood function of $\mathbf{O}, \mathbf{S}_{t+1}, \mathbf{D}$, given conditions \mathbf{C} and \mathbf{S}_t , summarized as:

$$\text{maximize } \log p(\mathbf{O}, \mathbf{S}_{t+1}, \mathbf{D} | \mathbf{C}, \mathbf{S}_t). \quad (10)$$

Based on the variational inference method, the likelihood lower bound of the Objective function could be obtained,

$$\begin{aligned} \log p(\mathbf{O}, \mathbf{S}_{t+1}, \mathbf{D} | \mathbf{C}, \mathbf{S}_t) &\geq L_{ELBO} \\ &= E_{q(\mathbf{Z}_t | \mathbf{S}_t) q(\mathbf{Z}^{do} | \mathbf{Z}_t, \mathbf{D})} [\log p(\mathbf{S}_{t+1} | \mathbf{Z}^{do}) + \log p(\mathbf{O} | \mathbf{Z}^{do}) + \\ &\quad \log p(\mathbf{D} | \mathbf{Z}_t, \mathbf{C})] - KL(q(\mathbf{Z}^{do} | \mathbf{Z}_t, \mathbf{D}) | p(\mathbf{Z}^{do} | \mathbf{Z}_t, \mathbf{D})) - \\ &\quad KL(q(\mathbf{Z}_t | \mathbf{S}_t) | p(\mathbf{Z}_t | \mathbf{S}_t)) \end{aligned} \quad (11)$$

where KL is the Kullback-Leibler divergence. In (11), the first 3 terms are the log-likelihood terms and the last two terms are the KL divergence terms. To maximize L_{ELBO} means maximizing the log-likelihood terms, which can be seen as regularization terms for the model, and minimizing KL divergence terms, which means making the prior distribution as close as possible to the posterior distribution.

IV. CASE STUDIES

A. Decision making for robot movement tasks

1) Problem description

The first case was robot movement simulation using OpenAI-Gym, which is an Open-Source physics platform for training and testing algorithms. This task required continuous manipulating of the robot end effector to reach a Objective position \mathbf{O} with coordinates (x, y, z) . The State variable \mathbf{S} , including the position of the robot end effector and poster of the robot arm, include measured images at corresponding times. Thus, the decision model makes Decision variable $\mathbf{D} = (D_1, D_2, D_3)$, i.e., action or movements of the end effector in three directions, based on current State variable \mathbf{S}_t represented by current image \mathbf{X}_t , until it reaches its destination \mathbf{O} .

The Shadow Objective variable selected the difference in distance $\mathbf{C} = (\delta x, \delta y, \delta z)$ between Objective coordinates and the current coordinates. Every time an action was made based on current \mathbf{X}_t and \mathbf{C} , the resulting image of the State after the

action was X_{t+1} . The position of the corresponding robot end effector in State image X_{t+1} was O' , i.e., the robot end effector moved to O' after executing D_t .

The robot was composed of seven elements V_t^1 to V_t^7 . Due to the difficulty in obtaining its polar coordinates, this research analyzed its motion law based on the Euler coordinate system. Based on the law of image data generated law, the relationship between the coordinates of end effector (e_t^1, e_t^2, e_t^3) and the seven elements of the robot can be represented in the graph shown in **Error! Reference source not found.** (a). B_t is the background feature, which is independent to other features and Objectives.

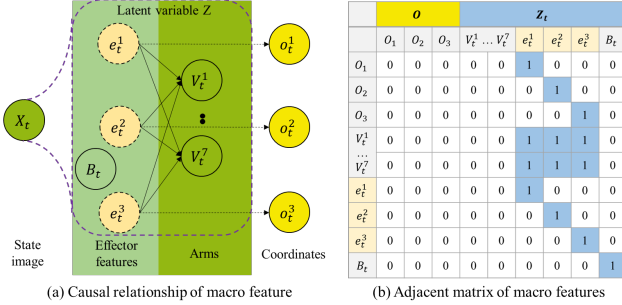


Fig. 5 Causal relationships and adjacent matrix of macro features in planning robot movement tasks.

2) Experiment setting

The proposed causal based decision making method (with no loop in its causal graph) (CDM-NL) was compared with two other methods: (i) a causal based decision making method with the loop in its causal graph (CDM-L), (ii) a pure data-driven decision making method without causal relationships (DM-NC). These methods were tested on four datasets, in which the input image X_t was added with Gaussian noise of 0, 0.1, 0.2, and 0.3, respectively.

The CDM-L only differs from the proposed method CDM-NL in that CDM-L had input from O , whilst CAM-NL had input from C , and the rest of the causal relation graph is the same. The DM-NC lacks a decision intervention module, the rest of the neural network structure is the same as the CDM-NL. The quality of decision making is evaluated by the mean squared error between Decisions D_{pre} made by model and the true Decision D_{lable} , as defined,

$$Error = \sqrt{|D_{lable} - D_{pre}|^2} \quad D \in R^3. \quad (12)$$

3) Analysis of experiment results

Fig. 6 illustrates the errors of the compared methods. It revealed that the method proposed in this research can maintain stable decision outputs despite the noises, whereas the decision making performance of the other methods had significant errors with increased noises.

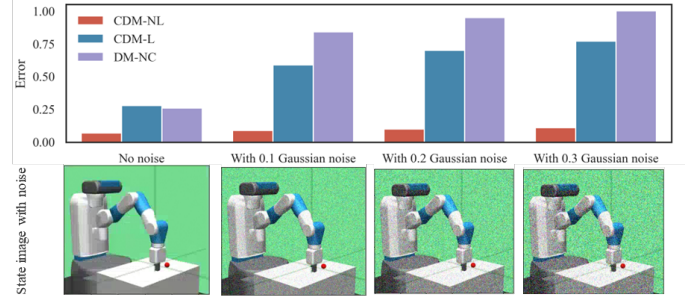


Fig. 6 Experiment results on different datasets of robot motion control task.

Furthermore, the errors of decision D_{pre} on a validation set with 0.3 Gaussian noises is analyzed. The error densities of three actions D_1, D_2, D_3 in decision D_{pre} is illustrated in Fig. 7 (a-c). It shows that the error distributions that the decision action errors of CDM-NL are concentrated within $[-0.2, 0.2]$. In contrast, the error distributions of CDM-L and DM-NC have a wider range. It indicates that the proposed method has a stable decision-making in noised environments.

Then, the effectiveness of introducing causal relationship is confirmed by assessing the independence of decision errors. Based on the relationship between the three positions of the robot and the three positions of the Objective in **Error! Reference source not found.**, the decision errors of D_1, D_2, D_3 should be independent of each other. To evaluate this, the Pearson Coefficients of errors between each pair of actions (D_1, D_2, D_3) of the three methods are calculated, and listed in **Error! Reference source not found.** It reveals that the Pearson Coefficients of errors of CDM-NL are all below 0.1, indicating independence among action errors. In contrast, the Pearson Coefficients of CDM-L and DM-NC are relatively large, implying dependencies (links) between decided actions.

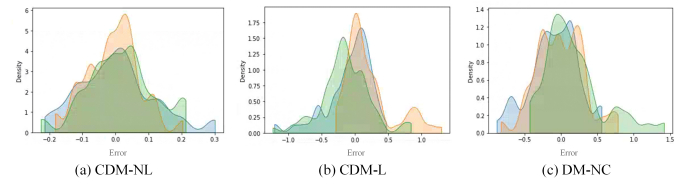


Fig. 7 Error densities of actions D_1, D_2, D_3 of decision D_{pre} .

These results show that the proposed method achieved effective decoupling, which is key factor contributing to its stability and accuracy in decision making. It is also suggested that poor decoupling of learning data is a significant factor in less stable decision making (with bigger errors).

TABLE 2
PEARSON COEFFICIENTS OF EACH PAIRS OF ACTIONS ERRORS

Pearson Coefficient	D_1, D_2	D_2, D_3	D_1, D_3
CDM-NL	0.08	0.05	0.04
CDM-L	0.07	0.18	0.33
DM-NC	0.24	0.18	0.35

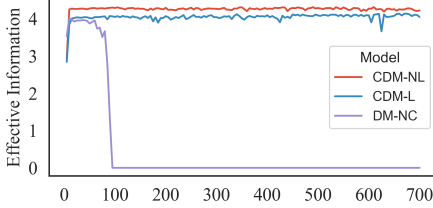
To further validate the benefits of employing causal relationships, the effective information (EI) from the output of

Decision to the predicted Objective coordinates was calculated. EI is a measure of causal effectiveness, and higher value indicate that the neural network can offer more causal information, as illustrated in (14).

$$EI = MI(\mathbf{O}, \mathbf{D}_t | do(\mathbf{D}_t = H^{max})) \quad (13)$$

where MI is the mutual information, H^{max} is the maximum entropy distribution of \mathbf{D}_t .

The EI of the three methods during the training process is



shown in

Fig. 8 Effective information of models in training process., it reveals that the methods incorporating causal relationships experienced a notable increase in EI , while the DM-NC basically remained around zero (not increased). In addition, CDM-NL shows a higher growth rate and final EI value compared with CDM-L, suggesting that models breaking loop can acquire more EI .

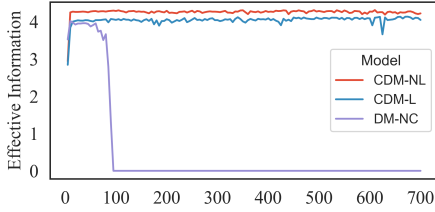


Fig. 8 Effective information of models in training process.

4) Comparison with reinforcement learning methods

Furthermore, the proposed method was compared with existing offline reinforcement learning algorithms, including Conservative Q-Learning (CQL) and Decision Transformer (DT) using the d3rlpy library [30] in noisy environments. The evaluation metric employed was the normalized cumulative reward over 50 test runs, where the reward at each time step was the negative Euclidean distance of the actuator from the target position, as shown below:

$$\text{normalized reward} = 100\% \times \frac{\text{reward} - \text{reward}_r}{\text{reward}_{best} - \text{reward}_r} \quad (14)$$

where reward_r is the reward of random action strategy, reward_{best} is the best reward in the three methods. The results are shown in TABLE 3.

TABLE 3
NORMALIZED REWARD OF THE METHODS

Method	No noise	0.1 Noise	0.2 Noise	0.3 Noise
CDM-NL	100	91.7	77.0	78.1
CQL	12.7	10.4	8.9	7.6
DT	12.1	7.3	6.3	12.0

It can be seen from TABLE 3, compared to CQL and DT, the proposed method not only achieved higher reward values

but also maintained robust decision-making performance in noisy environments.

B. Decision making for component deformation control during manufacturing

1) Problem description

In aircraft structural components manufacturing, it is important to minimize machining deformation, which is a critical industrial objective \mathbf{O} . The Decisions are made based on the current machining State variable \mathbf{S}_t of the components, which including data of deformation causes, including residual stress field $\boldsymbol{\sigma}_t$ and geometric \mathbf{G}_t . In this experiment, the deformation control Decision selected was the machining of 8 process-ribs ($r_1 - r_8$), as shown in Fig. 8. The Decision variable is represented as $\mathbf{D} = (D_1, \dots, D_8)$, which indicates whether these ribs are to be machined ($D_i = 0$) or reserved ($D_i = 1$) to manage residual stress. The Objectives variable \mathbf{O} was to minimize deformation (O_1, O_2, O_3, O_4) at four corners.

The Shadow Objective was the difference in deformation between current deformation and final deformation at the 4 corners, $\mathbf{C} = (\delta c_1, \delta c_2, \delta c_3, \delta c_4)$, where δc_i is deformation at corner i in Z direction. Following the Decision \mathbf{D} made for machining process-ribs, the subsequent State \mathbf{S}_{t+1} emerges.

Geometric data \mathbf{G} parameterized by a matrix, contains a significant amount of microscopic geometric elements. These elements are mixed with macroscopic geometric features with physical characteristics, such as process-ribs \mathbf{r}_t , and web \mathbf{w}_t , and stiffness \mathbf{B}_t . Those features are expressed by latent variable \mathbf{Z}_t . Based on the physical laws of deformation, there exist causal relationships among the macro features and physical characteristics, as illustrated in **Error! Reference source not found.**

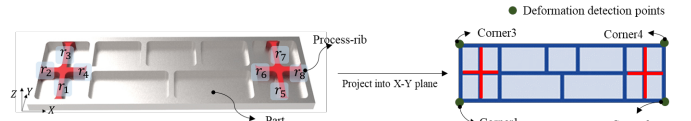


Fig. 9 Aircraft structural component with 8 process-ribs and 4 deformation detection points.

2) Experiment setting

The proposed method CDM-NL was compared with CDM-L and DM-NC in simulation environment. In the simulation environment, various components with different initial residual stress field $\boldsymbol{\sigma}$ were simulated under different machining operations (Decisions \mathbf{D} for machining process-ribs). The resulting machining deformation was considered as the Objective \mathbf{O} . Initially, CDM-NL, CDM-L and DM-NC were trained on a dataset with no residual stress noise. Then, to compare the stability, the three models were validated on datasets, where the residual stress with 0, 1MPa, 5MPa, and 10MPa noises, respectively. The quality of decision making was compared by the mean squared errors between the made Decisions \mathbf{D}_{pre} and labeled process data \mathbf{D}_{lable} :

$$\text{Error} = \sqrt{|\mathbf{D}_{lable} - \mathbf{D}_{pre}|^2} \quad \mathbf{D} \in \mathbb{R}^8. \quad (15)$$

3) Simulation experiment results

The Decisions errors of the three decision making methods are shown in Fig. 10. It can be seen from that the proposed method consistently demonstrates stability and accuracy across the 4 dataset. It should be noted here that Decision process D is a binary array, which theoretically has an error of 0.5 when it is uniformly random sampled, as shown by the red line in Fig. 10. Notably, all methods, except for the proposed one, are either close to or worse than random decision-making.

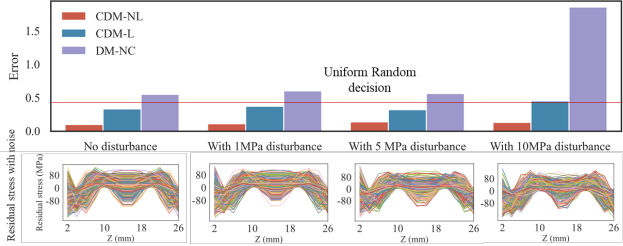


Fig. 10 Simulation results of the methods on 4 datasets.

Further analysis was conducted to determine whether latent variables Z learned the corresponding macro geometric features, i.e., decoupling ability. A comparison was made between the CDM-NL method and CDM-L method. The random manufacturing plans (Decision D) was applied in four cases, and the subsequent geometric data G_{t+1} reconstructed from the Decision-intervened macro geometry features Z_t^{do} was shown in Fig. 11.

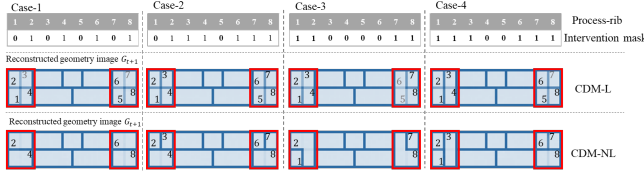


Fig. 11 Reconstructed geometry State G_{t+1} by random intervention on macro geometry variables.

Fig. 11 shows that by intervening in different latent variables, the proposed method can effectively remove the corresponding process-ribs in reconstructed geometry images. It proves that the proposed method decoupled macro variables of process-ribs from the high dimensional geometric data. It also enhances the interpretability of the model incorporating with causal knowledge, because it can provide a clearer causal relationship between different variables, leading to more explainable decisions. For example, in the CDM-NL method, it can explain why a particular decision was made, that is, the optimized deformation was achieved by changing the corresponding process-rib. It helps users better understand and trust the decision. However, the CDM-L method could not capture the macro geometry features, indicating that even if causal knowledge were introduced, it still would not be able to accurately learn the causal effect between variables with the existence of a loop structure in its causal graph.

To further validate the effectiveness of the introduced causal relationships in component deformation control, the EI of the model from Decision D (process plan for machining process-rib) to Objective O (deformation) was calculated. The EI changes of the three methods during the training process

are shown in Fig. 12. Similar to the robot movement task, the EI value of the methods considering causal relationships is higher than the method without considering causal relationships. Furthermore the EI value of the proposed method CDM-NL is larger than CDM-L. It indicated that the proposed method was more effective.

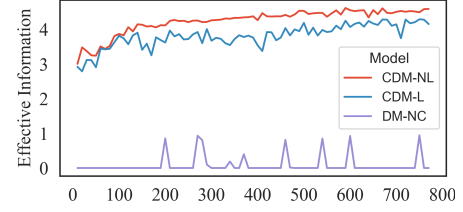


Fig. 12 Effective information of the three decision making methods in component deformation control.

4) Actual experiment results

To compare the different methods, the machined components should have same residual stress field, while the residual stress fields of components are different from each other, leading to comparison difficulty in actual machining environment. Therefore, this experiment was only used to further validate the effectiveness and stability of the proposed method. The decision making model of the proposed method trained on the simulation data (described in Section 4.2.3) was tested in the actual environment. Two aluminum alloy aircraft structural components with the same geometry but different residual stress distributions were used for the experiment. The size of the components is $636mm \times 180mm \times 26mm$, and the material is 7075 aluminum alloy.

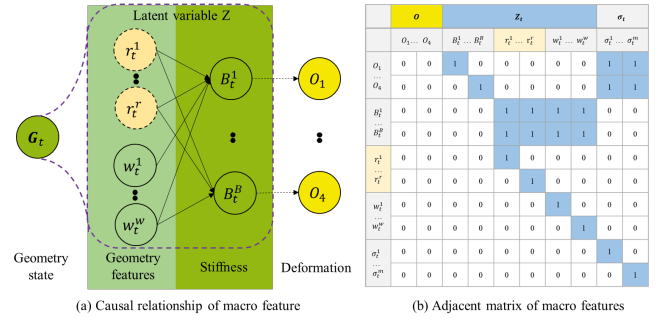


Fig. 13 Causal relationship and adjacent matrix of macro features from machining process decision-making task.

As illustrated in Fig. 14 (a), the two components were machined in the worktable with fixtures installed with sensors, which were used to measure forces and inference residual stress fields. The X-Y plane of each component was divided into 4 areas with residual stress along the Z direction. As shown in Fig. 14 (b), the residual stresses of each area is not smooth or even and its distribution was more complex than the simulation environment. For the two structural components, the process plans (Decision D) for machining process-ribs were $D_1 = [0, 1, 0, 1, 0, 1, 1, 1]$, and $D_2 = [0, 0, 0, 0, 1, 0, 0, 1]$.

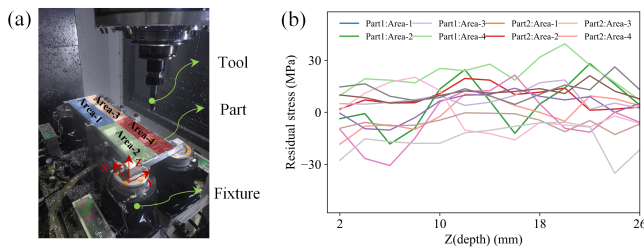


Fig. 14 Actual machining experiment. (a) Machining environment. (b) Residual stress fields of the two components.

To validate the applicability of the model trained in the simulation environment to the actual environment, the deformation prediction and control effectiveness of the proposed method were analyzed. The method's deformation prediction module was used to predict the machining deformation of the components after executing the machining process plans (Decision D) and compared it with the benchmark deformation (calculated using finite element analysis), as illustrated in **Error! Reference source not found.**

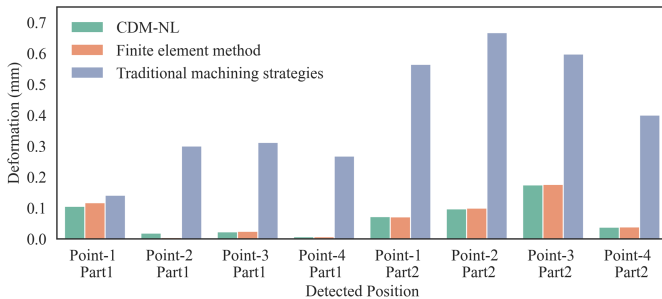


Fig. 15 Experiment results in the actual environment.

The root mean squared error was 0.006mm, which is close to the finite element model. It indicates that the proposed method was capable of making stable decisions in complex scenarios. The results were evaluated by experienced engineers from aerospace industry, and they compared with their existing machining practice and commented that the machining deformation of structural components was effectively controlled by the proposed method, and the average machining deformation reduction was around 0.34mm compared with current industrial machining capability.

V. CONCLUSIONS AND FURTHER WORK

Inefficient, unstable, and erroneous decision making are crucial challenge for application of data-driven methods in manufacturing environments with noises and changes, due to the learned correlations between State variables and Decision variables. This paper reported a causal-based decision making framework and tested on both simulation and actual cases. It was demonstrated that the causal-based decision making method maintained better stability for both continuous and discrete decision variables in complex and changing scenarios, compared with other data-driven methods. **Compared with non-causal methods, the proposed methods with causal knowledge achieved 74% and 70% improvements on decision making accuracy in noisy robot movement and deformation**

control task. In addition, in the actual deformation control experiments, the proposed method reduced deformation by 0.34mm compared with traditional methods.

Potential industrial applications include supply chain management, production planning, and equipment maintenance. These applications can lead to significantly reduced operational costs and improved product quality, highlighting the practical benefits and applicability of our research.

Future research aims to extract causal relationships autonomously using algorithms like causal discovery and causal emergence, to reduce the reliance on human knowledge. This opens the potential for collaborative decision-making between humans and machines, which could be more accurate and stable than decisions made by either party alone.

REFERENCES

- [1] A. Novak, D. Bennett, and T. Kliestik, "Product decision-making information systems, real-time sensor networks, and artificial intelligence-driven big data analytics in sustainable Industry 4.0," *Econ. Manag. Financ. Mark.*, vol. 16, no. 2, pp. 62–72, 2021.
- [2] T. Kliestik, E. Nica, H. Musa, M. Poliak, and E.-A. Mihai, "Networked, smart, and responsive devices in industry 4.0 manufacturing systems," *Econ. Manag. Financ. Mark.*, vol. 15, no. 3, pp. 23–29, 2020.
- [3] M. L. H Souza, C. A. da Costa, G. de Oliveira Ramos, and R. da Rosa Righi, "A survey on decision-making based on system reliability in the context of Industry 4.0," *J. Manuf. Syst.*, vol. 56, pp. 133–156, Jul. 2020.
- [4] S. P. Leo Kumar, "Knowledge-based expert system in manufacturing planning: state-of-the-art review," *Int. J. Prod. Res.*, vol. 57, no. 15–16, pp. 4766–4790, 2019.
- [5] E. Francelanza, J. Borg, and C. Constantinescu, "Development and evaluation of a knowledge-based decision-making approach for designing changeable manufacturing systems," *CIRP J. Manuf. Sci. Technol.*, vol. 16, pp. 81–101, Jan. 2017.
- [6] M. I. Boloş, I. A. Bradea, and C. Delcea, "A Fuzzy Logic Algorithm for Optimizing the Investment Decisions within Companies," *Symmetry* 2019, Vol. 11, Page 186, vol. 11, no. 2, p. 186, Feb. 2019, Accessed: Jul. 02, 2024.
- [7] X. Guan, Y. Wang, and L. Tao, "Machining scheme selection of digital manufacturing based on genetic algorithm and AHP," *J. Intell. Manuf.*, vol. 20, no. 6, pp. 661–669, Dec. 2009.
- [8] P. Renna, "A Decision Investment Model to Design Manufacturing Systems based on a genetic algorithm and Monte-Carlo simulation," *Int. J. Comput. Integr. Manuf.*, vol. 30, no. 6, pp. 590–605, Jun. 2017.
- [9] W. Xu and Y. Yin, "Functional objectives decision-making of discrete manufacturing system based on integrated ant colony optimization and particle swarm optimization approach," *Adv. Prod. Eng. Manag.*, vol. 13, no. 4, pp. 389–404, Dec. 2018.
- [10] C. Sun, "Research on investment decision-making model from the perspective of 'Internet of Things + Big data,'" *Futur. Gener. Comput. Syst.*, vol. 107, pp. 286–292, Jun. 2020.
- [11] J. Wang, Y. Sun, W. Zhang, I. Thomas, S. Duan, and Y. Shi, "Large-Scale Online Multitask Learning and Decision Making for Flexible Manufacturing," *IEEE Trans. Ind. Informatics*, vol. 12, no. 6, pp. 2139–2147, Dec. 2016.
- [12] M. Panzer and B. Bender, "Deep reinforcement learning in production systems: a systematic literature review," *Int. J. Prod. Res.*, vol. 60, no. 13, pp. 4316–4341, 2022.
- [13] F. Tao, Q. Qi, A. Liu, and A. Kusiak, "Data-driven smart manufacturing," *J. Manuf. Syst.*, vol. 48, pp. 157–169, 2018.
- [14] J. Wang, Y. Ma, L. Zhang, R. X. Gao, and D. Wu, "Deep learning for smart manufacturing: Methods and applications," *J. Manuf. Syst.*, vol. 48, pp. 144–156, 2018.
- [15] T. M. Moerland, J. Broekens, A. Plaat, and C. M. Jonker, "Model-based Reinforcement Learning: A Survey," *Found. Trends® Mach. Learn.*, vol. 16, no. 1, pp. 1–118, 2023.
- [16] M. Liu, M. Zhu, and W. Zhang, "Goal-Conditioned Reinforcement Learning: Problems and Solutions," *arXiv Prepr.*, pp. 1–10, Jan. 2022.

- [17] C. Liu, J. Ding, and J. Sun, "Reinforcement Learning Based Decision Making of Operational Indices in Process Industry under Changing Environment," *IEEE Trans. Ind. Informatics*, vol. 17, no. 4, pp. 2727–2736, Apr. 2021.
- [18] S. Emmons, B. Eysenbach, I. Kostrikov, and S. Levine, "RvS: What is Essential for Offline RL via Supervised Learning?," ICLR 2022, May 2021.
- [19] J. Schmidhuber, "Reinforcement Learning Upside Down: Don't Predict Rewards -- Just Map Them to Actions," *arXiv Prepr.*, pp. 1–22, Dec. 2019.
- [20] R. K. Srivastava, P. Shyam, F. Mutz, W. Jaśkowski, and J. Schmidhuber, "Training Agents using Upside-Down Reinforcement Learning," *arXiv Prepr.*, pp. 1–31, Dec. 2019.
- [21] J. G. Richens, C. M. Lee, and S. Johri, "Improving the accuracy of medical diagnosis with causal machine learning," *Nat. Commun.*, vol. 11, no. 1, Dec. 2020.
- [22] C. A. Escobar, M. E. McGovern, and R. Morales-Menendez, "Quality 4.0: a review of big data challenges in manufacturing," *J. Intell. Manuf.*, vol. 32, no. 8, pp. 2319–2334, Dec. 2021.
- [23] J. Li, Y. Wang, Y. Zi, H. Zhang, and C. Li, "Causal Consistency Network: A Collaborative Multimachine Generalization Method for Bearing Fault Diagnosis," *IEEE Trans. Ind. Informatics*, vol. 19, no. 4, pp. 5915–5924, Apr. 2023.
- [24] S. Marrow, E. J. Michaud, and E. Hoel, "Examining the causal structures of deep neural networks using information theory," *Entropy*, vol. 22, no. 12, pp. 1–14, 2020.
- [25] F. Eberhardt and L. L. Lee, "Causal Emergence: When Distortions in a Map Obscure the Territory," *Philosophies*, vol. 7, no. 2, Apr. 2022.
- [26] K. P. Murphy, *Probabilistic machine learning: an introduction*. MIT press, 2022.
- [27] K. Krauth, Y. Wang, and M. I. Jordan, "Breaking Feedback Loops in Recommender Systems with Causal Inference," *arXiv Prepr. arXiv2207.01616*, pp. 1–23, 2022.
- [28] G. Sugihara *et al.*, "Detecting Causality in Complex Ecosystems," *Science (80-.)*, vol. 338, no. 6106, pp. 496–500, 2012.
- [29] M. Yang, F. Liu, Z. Chen, X. Shen, J. Hao, and J. Wang, "CausalVAE: Disentangled Representation Learning via Neural Structural Causal Models," in *Conference on Computer Vision and Pattern Recognition*, Proceedings of the IEEE, 2021, pp. 9588–9597.
- [30] T. Seno and M. Imai, "d3rlpy: An Offline Deep Reinforcement Learning Library," *J. Mach. Learn. Res.*, vol. 23, pp. 1–20, Nov. 2021, Accessed: Jul. 11, 2024.